

Analytical gradient for geometry optimizations of $(\text{H}_2\text{O})_n^-$ clusters as described by the PM1 polarizable model

Tae Hoon Choi, Kenneth D. Jordan *

Department of Chemistry and the Center for Molecular and Materials Simulations, University of Pittsburgh, Pittsburgh, PA 15260, United States

ARTICLE INFO

Article history:

Received 31 July 2008

In final form 2 September 2008

Available online 6 September 2008

ABSTRACT

Expressions for the analytical gradients of the PM1 polarization model for describing the interaction of excess electrons with water clusters are reported. For the $(\text{H}_2\text{O})_{45}^-$ cluster, evaluation of the gradient by use of the analytical expressions lead to a factor of five speedup over numerical evaluation of the gradient.

© 2008 Elsevier B.V. All rights reserved.

1. Introduction

The interaction of excess electrons with water clusters has been the subject of numerous experimental and theoretical studies [1–21]. Recently, our group has derived [22] a family of one-electron polarization models for $(\text{H}_2\text{O})_n^-$ cluster systems by applying an adiabatic separation to our previously introduced quantum Drude model [23–29]. In the polarization model, the total energy of a $(\text{H}_2\text{O})_n^-$ cluster is given by the sum of the energy of the neutral water cluster as described by the distributed point polarizable site (DPP) water model [30] and the electron binding energy (EBE) calculated using a one-electron Hamiltonian including explicit polarization of the water monomers by the excess electron.

To date, analytical gradients have not been presented for the Drude or associated polarization potential approaches. As a result, geometry optimization using these approaches have been carried out numerically, and simulations have been carried out using the Monte Carlo rather than molecular dynamics algorithms [23–28]. For optimizing the geometries and for carrying out simulations of the dynamics of large $(\text{H}_2\text{O})_n^-$ clusters, analytical gradients are required. In this work, we present the expressions for analytical gradients of the PM1 polarization model [22] and apply these to optimize the geometries of clusters as large as $(\text{H}_2\text{O})_{45}^-$.

2. Theory

In the PM1 model, the energy of the anion is given as the sum of the energy of the neutral water cluster plus the electron binding energy obtained from a model Hamiltonian. The DPP water model employed in the PM1 model employs three point charges, three atom-centered, mutually interacting point polarizable sites, damped dispersion interactions between O atoms, and exponential

repulsive interactions between atoms of different monomers. The model Hamiltonian for the excess electron includes interactions of the electron with the three-point charges, the induced dipoles resulting from water–water induction, and monomer-centered short-range repulsive potentials. In addition, the Hamiltonian includes terms that allow for the polarization of the water monomers by the excess electron.

2.1. Model Hamiltonian

The model Hamiltonian for an excess electron interacting with a water cluster is given (in atomic units) by

$$\mathbf{H} = -\frac{1}{2}\nabla^2 - \sum_i \frac{Q_i}{r_i} + \sum_j \frac{\boldsymbol{\mu}_j \cdot \mathbf{r}_j}{r_j^3} f_{\text{ind}}(r_j) + V_{\text{rep}} - \sum_j \frac{\alpha}{2r_j^4} f_{\text{pol}}(r_j), \quad (1)$$

where the second and third terms correspond to the interactions of the electron with the DPP point charges and the induced dipoles from intermolecular induction, respectively, the fourth term accounts for the short-range repulsive interactions of the excess electron with each monomer, and the last term incorporates the polarization of the monomers by the excess electron. For water the polarizability is approximately isotropic, and the experimental value 1.45 \AA^3 of the isotropic polarizability of water is employed in Eq. (1). The electron–water polarization is described by point polarizable centers located at the M site of each monomer (The M site is located on the rotational axis, and displaced 0.25 \AA from the O atom toward the H atoms). In Eq. (1) μ_j is the induced dipole moment located at the M site of the j th molecule and obtained by a vector sum of the three atom-centered induced dipole moments on the monomer resulting from the electronic field from the other monomers. It should be noted that the ‘collapse’ of the three induced dipoles on each monomer to a single dipole is not essential, and is made simply for computational speed. $f_{\text{ind}}(r_j) = 1 - \exp(-b_1 r_j^2)$ and $f_{\text{pol}}(r_j) = (1 - \exp(-b_2 r_j^3))^2$ are factors that damp

* Corresponding author. Fax: +1 412 624 8611.

E-mail address: jordan@pitt.edu (K.D. Jordan).

the short-range interactions of the excess electron with the induced dipoles (due to intermolecular induction) and polarizable sites, respectively. The damping is required to remove the $r \rightarrow 0$ divergences in the resulting integrals. The calculated energies are relatively insensitive to the precise functional forms of the damping factors. V_{rep} is constructed using the procedure of Wang and Jordan [25] which closely follows the approach of Schnitker and Rossky [31]. The excess electron is described using a set of s and p Gaussian-type functions, both monomer-centered and floating, with the latter being located at the center of mass of the cluster.

2.2. Analytical gradient of the PM1 model

The analytical gradient of the energy associated with a closed-shell Hartree–Fock wavefunction can be written as [32]:

$$\frac{\partial E}{\partial \mathbf{R}} = \sum_{\mu\nu} P_{\mu\nu} \frac{\partial H_{\mu\nu}^{\text{core}}}{\partial \mathbf{R}} + \frac{1}{2} \sum_{\mu\nu\lambda\sigma} P_{\nu\mu} P_{\lambda\sigma} \frac{\partial \langle \mu\nu | \sigma\lambda \rangle}{\partial \mathbf{R}} - \sum_{\mu\nu} Q_{\mu\nu} \frac{\partial S_{\mu\nu}}{\partial \mathbf{R}}, \quad (2)$$

where \mathbf{P} is the density matrix defined in terms of the molecular orbital coefficients

$$P_{\mu\nu} = 2 \sum_a^{m/2} C_{\mu a} C_{\nu a}, \quad (3)$$

and \mathbf{Q} is the energy-weighted density matrix given by

$$Q_{\mu\nu} = 2 \sum_a^{m/2} \varepsilon_a C_{\mu a} C_{\nu a}. \quad (4)$$

In Eqs. (3) and (4), the sum is over the occupied orbitals and ε_a is an orbital energy. $H_{\mu\nu}^{\text{core}}$ is a matrix element of the one-electron core Hamiltonian,

$$H_{\mu\nu}^{\text{core}} = \left\langle \phi_\mu \left| -\frac{1}{2} \nabla^2 - \sum_\alpha \frac{Z_\alpha}{r_\alpha} \right| \phi_\nu \right\rangle, \quad (5)$$

and $S_{\mu\nu}$ is an overlap matrix element, $S_{\mu\nu} = \langle \phi_\mu | \phi_\nu \rangle$. Thus the gradient of the Hartree–Fock energy can be calculated using the molecular orbital energies and LCAO–MO coefficients, together with the derivatives of the core Hamiltonian, the overlap matrix, and the two-electron integrals, $\langle \mu\nu | \sigma\lambda \rangle = \langle \mu\nu | \sigma\lambda \rangle - \frac{1}{2} \langle \mu\lambda | \sigma\nu \rangle$.

For the adiabatic polarization potential model described in the previous section, only a single electron is considered explicitly, and the gradient for the ground electronic state of the excess electron may be expressed as

$$\frac{\partial E}{\partial \mathbf{R}} = \sum_{\mu\nu} P_{\mu\nu} \frac{\partial H_{\mu\nu}}{\partial \mathbf{R}} - \sum_{\mu\nu} Q_{\mu\nu} \frac{\partial S_{\mu\nu}}{\partial \mathbf{R}}, \quad (P_{\mu\nu} = C_{\mu 1} C_{\nu 1}, \quad Q_{\mu\nu} = \varepsilon_1 C_{\mu 1} C_{\nu 1}), \quad (6)$$

where the Hamiltonian matrix elements $H_{\mu\nu} = \langle \phi_\mu | \mathbf{H} | \phi_\nu \rangle$ have only one-electron contributions, and only a single orbital energy and associated orbital coefficient are required. In general, there can be more than one bound excess electron state, and the subscript ‘1’ on the orbital energy and coefficients refers to the ground anionic state. The derivative of the Hamiltonian matrix is

$$\frac{\partial H_{\mu\nu}}{\partial \mathbf{R}} = \left\langle \frac{\partial \phi_\mu}{\partial \mathbf{R}} \left| \mathbf{H} \right| \phi_\nu \right\rangle + \left\langle \phi_\mu \left| \mathbf{H} \right| \frac{\partial \phi_\nu}{\partial \mathbf{R}} \right\rangle + \left\langle \phi_\mu \left| \frac{\partial \mathbf{H}}{\partial \mathbf{R}} \right| \phi_\nu \right\rangle. \quad (7)$$

There are twelve derivatives associated with the x , y , z coordinates of the three atoms and of the M site, for each water molecule. The derivatives of the basis functions with respect to the coordinates associated with the M sites are zero as there are no basis functions located on the M sites. Hence the Pulay terms [33,34] only require derivatives with respect to the atomic coordinates.

Table 1

Nonzero derivatives of the Hamiltonian in the PM1 model for an excess electron interacting with a water cluster

Coordinate	$\partial V_{\text{pc}} / \partial \mathbf{R}$	$\partial V_{\text{rep}} / \partial \mathbf{R}$	$\partial V_{\text{ind}} / \partial \mathbf{R}$	$\partial V_{\text{pol}} / \partial \mathbf{R}$
$R = R_O$	0	$\partial V_{\text{rep}} / \partial R_O$	$\partial V_{\text{ind}} / \partial R_O$	0
$R = R_H$	$\partial V_{\text{pc}} / \partial R_H$	$\partial V_{\text{rep}} / \partial R_H$	$\partial V_{\text{ind}} / \partial R_H$	0
$R = R_M$	$\partial V_{\text{pc}} / \partial R_M$	0	$\partial V_{\text{ind}} / \partial R_M$	$\partial V_{\text{pol}} / \partial R_M$

The nonzero contributions to the gradients of the Hamiltonian (i.e., the third term in Eq. (7)) are summarized in Table 1, where V_{pc} involves the interaction of the excess electron with the point charges of the DPP water model, and V_{ind} and V_{pol} correspond to the third and fifth terms in Eq. (1).

The greatest challenge in evaluating the gradients in the PM1 model is presented by the terms involving the interaction of the excess electron with the induced dipoles resulting from intermolecular induction. This term may be expanded as

$$\begin{aligned} \left\langle \phi_\mu \left| \frac{\partial V_{\text{ind}}}{\partial \mathbf{R}} \right| \phi_\nu \right\rangle &= \left\langle \phi_\mu \left| \frac{\partial}{\partial \mathbf{R}} \left[\sum_k \frac{\mathbf{r}_k}{r_k^3} \left(1 - e^{-br_k^2} \right) \right] \right| \phi_\nu \right\rangle \cdot \boldsymbol{\mu}_k \\ &+ \left\langle \phi_\mu \left| \sum_k \frac{\mathbf{r}_k}{r_k^3} \left(1 - e^{-br_k^2} \right) \right| \phi_\nu \right\rangle \cdot \frac{\partial \boldsymbol{\mu}_k}{\partial \mathbf{R}}, \end{aligned} \quad (8)$$

where \mathbf{r}_k is the vector from the electron to the induced dipole $\boldsymbol{\mu}_k$ located on the M site associated with molecule k , and use has been made of the fact that in the current implementation of the PM1 model, the intermolecular induced dipole moment vector is independent of the electron coordinates. The derivative of the first term in Eq. (8) depends only on the M site, but the derivative of the induced dipole moments in the second term depends on both the atomic sites and the M site. The procedure for calculating the derivatives of the induced dipole moments is discussed in the next section.

2.3. Derivative of the induced dipole moment

The induced dipole moment at atomic site i resulting from the interactions with the charges on the other monomers is given by [35]:

$$\boldsymbol{\mu}_i = \alpha_i \left(\mathbf{E}_i^0 + \sum_{j \neq i} \tilde{\mathbf{T}}_{ij} \cdot \boldsymbol{\mu}_j \right), \quad (9)$$

where \mathbf{E}_i^0 is the electric field at site i produced by the fixed charges on the other monomers, α_i is the polarizability of site i , and $\tilde{\mathbf{T}}_{ij}$ is the dipole tensor

$$\mathbf{E}_i^0 = \sum_{j \neq i} \frac{q_j \mathbf{R}_{ij}}{R_{ij}^3} f_1(R_{ij}), \quad \tilde{\mathbf{T}}_{ij} = \frac{1}{R_{ij}^3} \left(3 \mathbf{R}_{ij} \mathbf{R}_{ij} f_2(R_{ij}) - f_1(R_{ij}) \right). \quad (10)$$

In Eq. (10), $f_1(R_{ij})$ and $f_2(R_{ij})$ are damping functions used in the DPP water model. The induced dipoles are calculated iteratively.

The derivatives of the induced dipole moments are evaluated by differentiating Eq. (9):

$$\frac{\partial \boldsymbol{\mu}_i}{\partial \mathbf{R}_k} = \alpha_i \frac{\partial \mathbf{E}_i^0}{\partial \mathbf{R}_k} + \alpha_i \sum_{j \neq i} \frac{\partial \tilde{\mathbf{T}}_{ij}}{\partial \mathbf{R}_k} \cdot \boldsymbol{\mu}_j + \alpha_i \sum_{j \neq i} \tilde{\mathbf{T}}_{ij} \cdot \frac{\partial \boldsymbol{\mu}_j}{\partial \mathbf{R}_k}. \quad (11)$$

The derivatives in Eq. (11) could be solved iteratively, but this would require 12N SCF procedures, and it is computationally faster to use the inverse matrix approach, i.e., rewriting Eq. (11) as

$$\tilde{\mathbf{M}} \frac{\partial \boldsymbol{\mu}_i}{\partial \mathbf{R}_k} = \mathbf{C}_k, \quad \frac{\partial \boldsymbol{\mu}_i}{\partial \mathbf{R}_k} = \tilde{\mathbf{M}}^{-1} \mathbf{C}_k \quad (12)$$

Table 2
CPU time (s) to evaluate the energy and gradient of the $(\text{H}_2\text{O})_{45}^-$ cluster

Term ^a	CPU time(s)		
	Pulay	Non-Pulay	Total
$\frac{\partial V_{\text{NN}}}{\partial \mathbf{R}}$	N/A	0.7	0.7
$\frac{\partial s_{\mu\nu}}{\partial \mathbf{R}}$	4.1	N/A	4.1
$\frac{\partial (V_{\text{kin}})_{\mu\nu}}{\partial \mathbf{R}}$	12.6	N/A	12.6
$\frac{\partial (V_{\text{pc}})_{\mu\nu}}{\partial \mathbf{R}}$	28.8	11.7	40.5
$\frac{\partial (V_{\text{rep}})_{\mu\nu}}{\partial \mathbf{R}}$	39.0	27.8	66.8
$\frac{\partial \mu}{\partial \mathbf{R}}$	N/A	3.0	3.0
$\frac{\partial (V_{\text{ind}})_{\mu\nu}}{\partial \mathbf{R}}$	58.0	59.2	117.2
$\frac{\partial (V_{\text{pol}})_{\mu\nu}}{\partial \mathbf{R}}$	56.6	91.8	148.4 ^b
Total	199.1	194.2	393.3
Energy			35.8

^a $\frac{\partial (A)_{\mu\nu}}{\partial \mathbf{R}}$ is a shorthand notation of $\langle \frac{\partial \phi_{\mu}}{\partial \mathbf{R}} | A | \phi_{\nu} \rangle + \langle \phi_{\mu} | A | \frac{\partial \phi_{\nu}}{\partial \mathbf{R}} \rangle + \langle \phi_{\mu} | \frac{\partial A}{\partial \mathbf{R}} | \phi_{\nu} \rangle$.

^b The tabulated results are for a six *d* Gaussian function representation of the polarization potential. The total time to evaluate the $\frac{\partial (V_{\text{pol}})_{\mu\nu}}{\partial \mathbf{R}}$ contributions is reduced from 148.4 to 31.3 s if a three *s* GTF fit is used in place of the six *d* GTF fit. The CPU time for the energy evaluation is reduced from 35.8 to 17.1 s.

where \mathbf{C}_k is $9N$ component vector, and $\tilde{\mathbf{M}}$ is a $9N \times 9N$ matrix:

$$\tilde{\mathbf{M}} = \begin{pmatrix} -1 & 0 & 0 & \alpha_1 T_{12xx} & \alpha_1 T_{12xy} & \alpha_1 T_{12xz} & \cdots \\ 0 & -1 & 0 & \alpha_1 T_{12yx} & \alpha_1 T_{12yy} & \alpha_1 T_{12yz} & \cdots \\ 0 & 0 & -1 & \alpha_1 T_{12zx} & \alpha_1 T_{12zy} & \alpha_1 T_{12zz} & \cdots \\ \alpha_2 T_{21xx} & \alpha_2 T_{21xy} & \alpha_2 T_{21xz} & -1 & 0 & 0 & \cdots \\ \alpha_2 T_{21yx} & \alpha_2 T_{21yy} & \alpha_2 T_{21yz} & 0 & -1 & 0 & \cdots \\ \alpha_2 T_{21zx} & \alpha_2 T_{21zy} & \alpha_2 T_{21zz} & 0 & 0 & -1 & \cdots \\ \alpha_3 T_{31xx} & \alpha_3 T_{31xy} & \alpha_3 T_{31xz} & \alpha_3 T_{32xx} & \alpha_3 T_{32xy} & \alpha_3 T_{32xz} & \cdots \\ \alpha_3 T_{31yx} & \alpha_3 T_{31yy} & \alpha_3 T_{31yz} & \alpha_3 T_{32yx} & \alpha_3 T_{32yy} & \alpha_3 T_{32yz} & \cdots \\ \alpha_3 T_{31zx} & \alpha_3 T_{31zy} & \alpha_3 T_{31zz} & \alpha_3 T_{32zx} & \alpha_3 T_{32zy} & \alpha_3 T_{32zz} & \cdots \\ \vdots & \vdots & \vdots & \vdots & \vdots & \vdots & \ddots \end{pmatrix} \quad (13)$$

where N is the number of monomers, and $T_{ijxx}, T_{ijxy}, T_{ijxz}, \dots, T_{ijzz}$ are the nine elements of the dipole tensor, $\tilde{\mathbf{T}}_{ij}$. Once available, the inverse of $\tilde{\mathbf{M}}$ can be used for calculating the derivative of the induced dipole moments with respect to any degree of freedom.

The \mathbf{C}_k vector is expressed as

$$\mathbf{C}_k = \begin{pmatrix} -\alpha_1 \sum_{j \neq 1} \left(\frac{\partial E_{1x}^0}{\partial \mathbf{R}_k} + \frac{\partial T_{1jxx}}{\partial \mathbf{R}_k} \mu_{jx} + \frac{\partial T_{1jxy}}{\partial \mathbf{R}_k} \mu_{jy} + \frac{\partial T_{1jxz}}{\partial \mathbf{R}_k} \mu_{jz} \right) \\ -\alpha_1 \sum_{j \neq 1} \left(\frac{\partial E_{1y}^0}{\partial \mathbf{R}_k} + \frac{\partial T_{1jyx}}{\partial \mathbf{R}_k} \mu_{jx} + \frac{\partial T_{1jyy}}{\partial \mathbf{R}_k} \mu_{jy} + \frac{\partial T_{1jyz}}{\partial \mathbf{R}_k} \mu_{jz} \right) \\ -\alpha_1 \sum_{j \neq 1} \left(\frac{\partial E_{1z}^0}{\partial \mathbf{R}_k} + \frac{\partial T_{1jzx}}{\partial \mathbf{R}_k} \mu_{jx} + \frac{\partial T_{1jzy}}{\partial \mathbf{R}_k} \mu_{jy} + \frac{\partial T_{1jzz}}{\partial \mathbf{R}_k} \mu_{jz} \right) \\ -\alpha_2 \sum_{j \neq 2} \left(\frac{\partial E_{2x}^0}{\partial \mathbf{R}_k} + \frac{\partial T_{2jxx}}{\partial \mathbf{R}_k} \mu_{jx} + \frac{\partial T_{2jxy}}{\partial \mathbf{R}_k} \mu_{jy} + \frac{\partial T_{2jxz}}{\partial \mathbf{R}_k} \mu_{jz} \right) \\ -\alpha_2 \sum_{j \neq 2} \left(\frac{\partial E_{2y}^0}{\partial \mathbf{R}_k} + \frac{\partial T_{2jyx}}{\partial \mathbf{R}_k} \mu_{jx} + \frac{\partial T_{2jyy}}{\partial \mathbf{R}_k} \mu_{jy} + \frac{\partial T_{2jyz}}{\partial \mathbf{R}_k} \mu_{jz} \right) \\ -\alpha_2 \sum_{j \neq 2} \left(\frac{\partial E_{2z}^0}{\partial \mathbf{R}_k} + \frac{\partial T_{2jzx}}{\partial \mathbf{R}_k} \mu_{jx} + \frac{\partial T_{2jzy}}{\partial \mathbf{R}_k} \mu_{jy} + \frac{\partial T_{2jzz}}{\partial \mathbf{R}_k} \mu_{jz} \right) \\ \vdots \end{pmatrix}, \quad (14)$$

where E_{ix}^0, E_{iy}^0 , and E_{iz}^0 are the components of the electric field at site *i* produced by the fixed charges, and μ_x, μ_y , and μ_z are the components of the induced dipole moments, $\boldsymbol{\mu}$.

In the paper of Sommerfeld et al. [22] four different polarization potentials were presented. In this work we have adopted the PM1 model in which the undamped polarization potential terms are of the form $\alpha/2r_k^4$. The integrals involving the $\alpha/2r_k^4$ operator cannot be done analytically. To overcome this difficulty, the polarization operator associated with each monomer, including the associated damping factor, can be least squares fit to Gaussian-type functions (GTF) centered at the M site to give [22]:

$$V_{\text{pol}} \simeq - \sum_k a_k \text{GTF}_k, \quad (15)$$

where the a_k are the coefficients of the fit. The analytical derivatives of this term are straightforward to evaluate. In Ref. [22] the fit made use of six *d*-type Gaussians. This fit, together with a smaller three *s*-type Gaussian fit, will be used in the calculations presented in this paper. Moreover, because the polarization potentials in the four polarization models of Ref. [22] are all fit to GTF's, the gradient program works without change with all four models.

2.4. Treatment of constraints

The PM1 electron–water model is based on the DPP rigid monomer water model. Although Euler angle coordinates are commonly used for maintaining the geometrical constraints in such models, we have opted instead to use Cartesian coordinates in evaluating the gradients both due to the difficulties posed by the M site for an Euler angle representation and because of our plans to transition to a flexible monomer model in the future. The rigid monomer constraints were then imposed by transforming the derivatives from Cartesian coordinates to the Euler angle coordinates, ϕ, θ , and ψ .

For a given monomer, the derivatives in Euler angle coordinates corresponding to the translations are associated with the sum of the derivatives in Cartesian coordinates of the various atomic sites. The derivatives for the rotations in Euler angle coordinates are described by using the torque vector with respect to the centers of mass (CM) of the monomers [36]

$$\boldsymbol{\tau}_i = \Delta \mathbf{R}_{\text{O}_i} \times \mathbf{F}_{\text{O}_i} + \Delta \mathbf{R}_{\text{H}_{1i}} \times \mathbf{F}_{\text{H}_{1i}} + \Delta \mathbf{R}_{\text{H}_{2i}} \times \mathbf{F}_{\text{H}_{2i}} + \Delta \mathbf{R}_{\text{M}_i} \times \mathbf{F}_{\text{M}_i} \quad (16)$$

where \mathbf{F}_{O} , \mathbf{F}_{H} , and \mathbf{F}_{M} represent the forces at the O atom, a H atom, and M site, respectively, and $\Delta \mathbf{R}_{\text{O}_i}$ is the displacement vector given by $\mathbf{R}_{\text{O}_i} - \mathbf{R}_{\text{CM}_i}$, with $\Delta \mathbf{R}_{\text{H}_{1i}}$, $\Delta \mathbf{R}_{\text{H}_{2i}}$, and $\Delta \mathbf{R}_{\text{M}_i}$ being calculated in an analogous manner. The derivatives with respect to ϕ, θ , and ψ are then given by

$$\begin{pmatrix} \partial E / \partial \mathbf{R}_{i\phi} \\ \partial E / \partial \mathbf{R}_{i\theta} \\ \partial E / \partial \mathbf{R}_{i\psi} \end{pmatrix} = \begin{pmatrix} 0 & 0 & 1 \\ -\sin \phi & \cos \phi & 0 \\ \sin \theta \cos \phi & \sin \theta \sin \phi & \cos \theta \end{pmatrix} \begin{pmatrix} -\tau_{ix} \\ -\tau_{iy} \\ -\tau_{iz} \end{pmatrix} \quad (17)$$

3. Performance

In implementing the gradients of the PM1 model, care was taken to identify contributions that are zero or are related to other contributions, and to exploit this information to minimize the computational time. In order to check the efficiency of the analytical gradient code, it is instructive to compare timings with those for numerical evaluation of the gradients. The numerical gradients were evaluated both in a ‘brute force’ manner which requires $12N$ times more CPU time than a single-point energy evaluation, and by a ‘modified’ implementation that evaluates only those integrals that are changed upon specific displacements. It should be noted that numerical geometry optimizations in most *ab initio* electronic structure codes require $9N$ times more CPU time than single-point energy calculations as all integrals are evaluated for each atomic displacement.

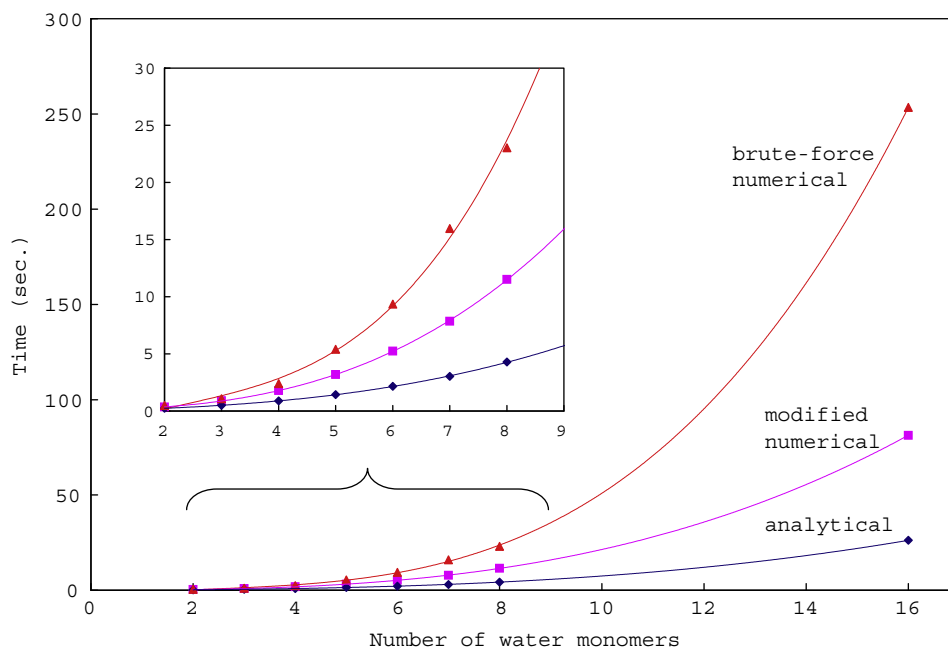


Fig. 1. Time required to calculate the gradient in one optimization step for several water cluster anions as described by the PM1/DPP model. The calculations were carried out on a 2.6 GHz opteron CPU.

Fig. 1 compares the computational time to calculate numerically and analytically the gradients for several water cluster anions. For a $(\text{H}_2\text{O})_{16}^-$ cluster, the evaluation of the gradient analytically is roughly nine times faster than the 'brute force' numerical gradient and three times faster than the modified numerical gradient. For the $(\text{H}_2\text{O})_{45}^-$ cluster, analytical evaluation of the gradient is fifty times faster than the 'brute force' numerical gradient and about five times faster than using the modified numerical evaluation of the gradient. With this speedup, optimization of the geometries of various isomers of a cluster the size of $(\text{H}_2\text{O})_{45}^-$ can be rapidly accomplished, but with our standard Gaussian-type orbital (GTO) basis set, which employs both monomer-centered and additional functions at the center of mass, the time to evaluate the gradient is still too long to permit long-time molecular dynamics simulations. Specifically, for $(\text{H}_2\text{O})_{45}^-$, our standard GTO basis set contains 287 primitive functions, and a single-point energy calculation takes 36 s, and the corresponding gradient requires 393 s on a 2.6 GHz opteron processor (see Table 2). There are several strategies for reducing the CPU time required for both the energy and gradient evaluations. These include (1) using a three *s* GTF rather than a six *d* GTF fit of the polarization potentials, (2) prescreening integrals and evaluating only those that are estimated to be greater in magnitude than some threshold, (3) combining the repulsive and polarization potential, and (4) replacing the present atom-centered basis set with a 3D grid of *s* Gaussians, which would eliminate the Pulay terms. Through a combination of these strategies, it should be possible to reduce the CPU time for a gradient evaluation of a cluster the size of $(\text{H}_2\text{O})_{45}^-$ as described by the PM1 model by as much as a factor of 50, which would permit long-time MD simulations. For example, we have found that use of a $6 \times 6 \times 6$ grid of *s* Gaussians rather than the present monomer-centered $+5s4p$ floating set of GTO's gives accurate electron binding energies for $(\text{H}_2\text{O})_{45}^-$ while resulting in a five-fold reduction in the CPU time required for the analytical gradient compared to that required with our standard GTO basis set.

4. Conclusions

Analytical gradients have been implemented for the PM1 model for $(\text{H}_2\text{O})_n^-$ clusters. The PM1 model is based on the DPP water model and allows for both intramolecular induction and polarization of the water molecule by the excess electron. The availability of analytical gradients will greatly facilitate use of the PM1 model in carrying out molecular dynamics simulations on large $(\text{H}_2\text{O})_n^-$ clusters. When the six *d* GTF representation of the polarization potential is used, the derivatives involving this term are the most time-consuming part of the calculation. With the smaller three *s* GTF fit to the polarization potential, the most time-consuming step in the gradient evaluation is due to the terms involving the interaction of the excess electron with the induced dipoles from intermolecular induction. We note also that with our standard monomer-centered basis set, about one half of the time of the gradient evaluation is due to the Pulay terms. By switching to a $6 \times 6 \times 6$ grid of *s* GTF functions for the electronic basis set, the Pulay terms are eliminated and the CPU time required to evaluate the analytical gradient for a cluster the size of $(\text{H}_2\text{O})_{45}^-$ is reduced about five-fold. With the adoption of the smaller three *s* GTF fit of the polarization potential and the use of the $6 \times 6 \times 6$ grid of *s* GTFs for the basis set, MD simulations for tens of psec. are feasible for clusters of this size when carried out on a single CPU, and for a few nsec. when carried out in parallel.

Acknowledgements

The authors acknowledge helpful discussions with Drs. Albert DeFusco, Thomas Sommerfeld, and Jack Simons. This research was carried out with support from the National Science Foundation, under Grant CHE518253.

References

- [1] D.H. Paik, I.R. Lee, D.S. Yang, J.S. Baskin, A.H. Zewail, *Science* 306 (2004) 672.
- [2] N.I. Hammer, J.W. Shin, J.M. Headrick, E.G. Kiden, J.R. Roscioli, G.H. Weddle, M.A. Johnson, *Science* 306 (2004) 675.
- [3] K.D. Jordan, *Science* 306 (2004) 618.

- [4] D. Borgis, P.J. Rossky, L. Turi, *J. Chem. Phys.* 125 (2006) 064501.
- [5] J.V. Coe et al., *J. Chem. Phys.* 92 (1990) 3980.
- [6] H. Haberland, H.G. Schindler, D.R. Worsnop, *Ber. Bunsen-Ges. Phys. Chem.* 88 (1984) 270.
- [7] J.R.R. Verlet, A.E. Bragg, A. Kammrath, O. Cheshnovsky, D.M. Neumark, *Science* 307 (2005) 93.
- [8] A.E. Bragg, J.R.R. Verlet, A. Kammrath, O. Cheshnovsky, D.M. Neumark, *Science* 306 (2004) 669.
- [9] M.H. Lee, B.S. Suh, K.S. Kim, *J. Chem. Phys.* 118 (2003) 9981.
- [10] M. Gutowski, P. Skurski, *Recent Res. Dev. Phys. Chem.* 3 (1999) 245.
- [11] M.J. Herbert, M. Head-Gordon, *J. Phys. Chem. A* 109 (2005) 5217.
- [12] M.J. Herbert, M. Head-Gordon, *Phys. Chem. Chem. Phys.* 8 (2006) 68.
- [13] N.I. Hammer, J.R. Roscioli, M.A. Johnson, E.M. Myshakin, K.D. Jordan, *J. Phys. Chem. A* 109 (2005) 11526.
- [14] N.I. Hammer, J.R. Roscioli, M.A. Johnson, *J. Phys. Chem. A* 109 (2005) 7896.
- [15] J.R. Roscioli, N.I. Hammer, M.A. Johnson, K. Diri, K.D. Jordan, *J. Chem. Phys.* 128 (2008) 104314.
- [16] N.I. Hammer, J.R. Roscioli, J.C. Bopp, J.M. Headrick, M.A. Johnson, *J. Chem. Phys.* 123 (2005) 244311.
- [17] J.R. Roscioli, M.A. Johnson, *J. Chem. Phys.* 126 (2007) 024307.
- [18] R.N. Barnett, U. Landman, C.L. Cleveland, J. Jortner, *J. Chem. Phys.* 88 (1988) 4429.
- [19] L. Turi, W.S. Sheu, P.J. Rossky, *Science* 309 (2005) 914.
- [20] L. Turi, A. Madarasz, P.J. Rossky, *J. Chem. Phys.* 125 (2006) 014308.
- [21] T. Frigato, J. VandeVondele, B. Schmidt, C. Schutte, P. Jungwirth, *J. Phys. Chem. A* 10 (2008) 1021.
- [22] T. Sommerfeld, A. DeFusco, K.D. Jordan, *J. Phys. Chem. A*, in press.
- [23] F. Wang, K.D. Jordan, *J. Chem. Phys.* 114 (2001) 10717.
- [24] F. Wang, K.D. Jordan, *J. Chem. Phys.* 116 (2002) 6973.
- [25] F. Wang, K.D. Jordan, *J. Chem. Phys.* 119 (2003) 11645.
- [26] T. Sommerfeld, K.D. Jordan, *J. Phys. Chem. Phys. A* 109 (2005) 11531.
- [27] T. Sommerfeld, K.D. Jordan, *J. Am. Chem. Soc.* 128 (2006) 5828.
- [28] T. Sommerfeld, S.D. Gardner, A. DeFusco, K.D. Jordan, *J. Chem. Phys.* 125 (2006) 174301.
- [29] A. DeFusco, T. Sommerfeld, K.D. Jordan, *Chem. Phys. Lett.* 455 (2008) 135.
- [30] A. DeFusco, D. Schofield, K.D. Jordan, *Mol. Phys.* 105 (2007) 2681.
- [31] J. Schnitker, P.J. Rossky, *J. Chem. Phys.* 86 (1987) 3462.
- [32] A. Szabo, N.S. Ostlund, *Modern Quantum Chemistry: Introduction to Advanced Electronic Structure Theory*, McGraw-Hall Publishing Company, New York, 1989.
- [33] P. Pulay, *Mol. Phys.* 17 (1969) 197.
- [34] W. Meyer, P. Pulay, *J. Chem. Phys.* 56 (1972) 2109.
- [35] L.X. Dang, T.-M. Chang, *J. Chem. Phys.* 106 (19) (1997) 8149.
- [36] H. Goldstein, *Classical Mechanics*, Addison-Wesley, Massachusetts, 1980.